Materials Chemistry and Physics 277 (2022) 125504

Contents lists available at ScienceDirect

Materials Chemistry and Physics

journal homepage: www.elsevier.com/locate/matchemphys

Effect of pH on the removal of anionic and cationic dyes using zinc curcumin oxide nanoparticles as adsorbent

Celine Arab, Riham El Kurdi, Digambara Patra *

Department of Chemistry, American University of Beirut, Beirut, Lebanon

HIGHLIGHTS

- Zinc curcumin oxide nanoparticles were synthesized and used as adsorbent.
- Congo red had the highest adsorption capacity in acidic medium.
- Methylene blue, rhodamine 6G and rhodamine B had highest adsorption capacity in basic solutions.
- Even though methyl orange is anionic, it was adsorbed better in basic medium.
- All the adsorption processes studied followed a pseudo-second order kinetic model.

GRAPHICAL ABSTRACT

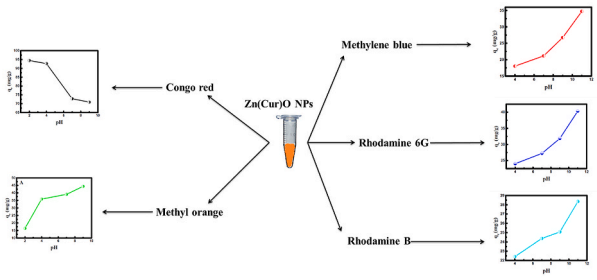

ARTICLE INFO

Keywords:
Anionic dyes
Cationic dyes
Zn(cur)O NPs
Adsorption
pH
Adsorption capacity
Kinetics

ABSTRACT

Recently, organic dyes are highly found in wastewater because of the plastic, painting, cosmetics, paper, leather, and food industries. They are dangerous and can affect the environment in addition to the human beings. Many methods were studied in order to get rid of them. Among all the techniques, adsorption was determined to be a successful, economic, ecofriendly, and efficient one. Zinc oxide nanoparticles were complexed with curcumin in order to generate zinc curcumin oxide nanoparticles that will be used as adsorbent. The efficiency of zinc curcumin oxide nanoparticles as adsorbent was investigated for different organic dyes such as congo red (CR), methyl orange (MO), methylene blue (MB), rhodamine 6G (Rh6G), and rhodamine B (RhB). The effect of pH was investigated in this study for the diverse anionic and cationic dyes. The highest adsorption capacities q_e of the dyes were determined for CR, MO, MB, Rh6G, and RhB to be 94.54, 44.38, 34.71, 38.184, and 28.34 mg/g respectively. Only congo red had the highest adsorption capacity at an acidic pH while the other dyes had the highest adsorption capacity at a basic pH. In addition, all the adsorption processes that were studied followed a pseudo-second order kinetic model.

1. Introduction

Nowadays, organic dyes have gained much importance due to their usage in different types of industries such as leather, plastic, textile, paints, cosmetics, paper, and food production [1,2]. These dyes are significantly present in wastewater and can cause a danger to human beings [2]. They are considered as pollutants that can bring out a risk to the environment. By breakdown and decomposition, they are prone to form carcinogenic and mutagenic compounds due to their high toxicity [1]. Numerous techniques have been applied until now, such as

* Corresponding author.
E-mail address: dp03@aub.edu.lb (D. Patra).

https://doi.org/10.1016/j.matchemphys.2021.125504
Received 1 March 2021; Received in revised form 16 July 2021; Accepted 27 November 2021
Available online 29 November 2021

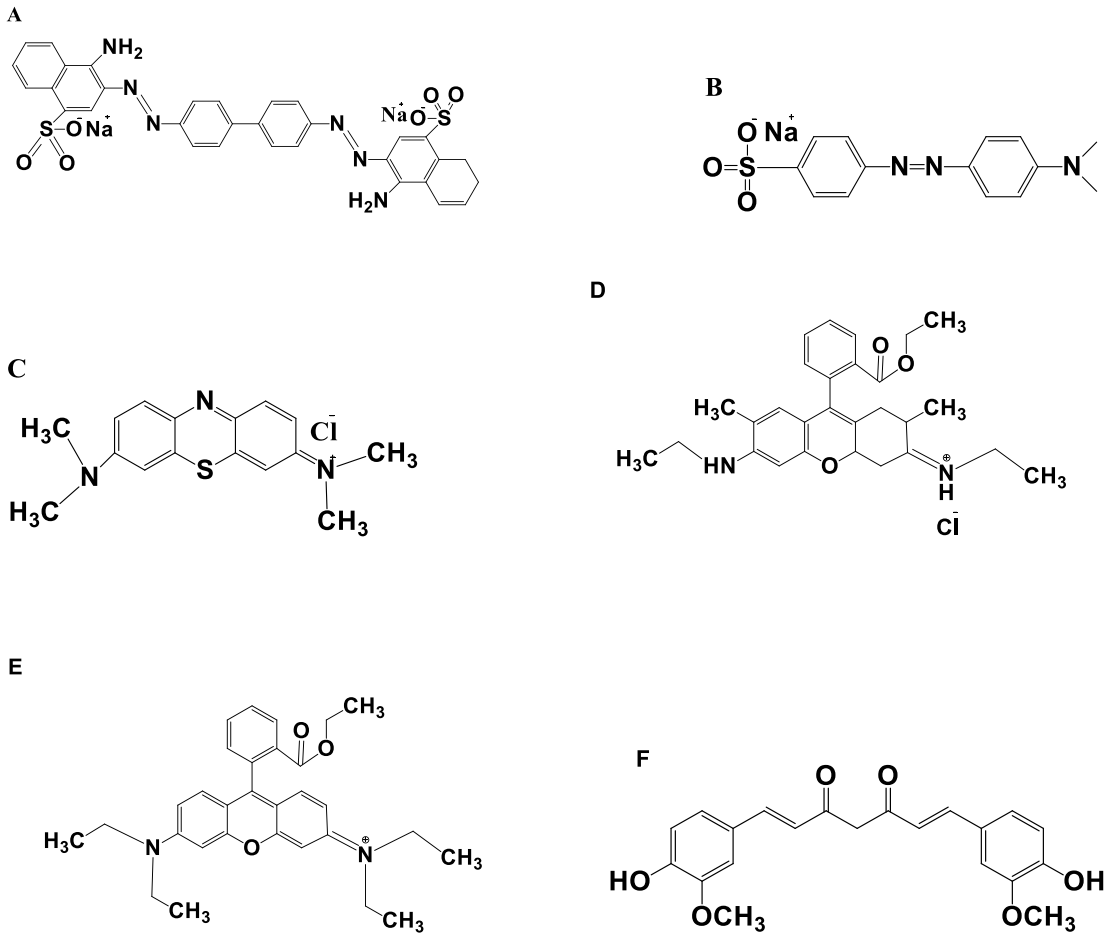

Fig. 1. Chemical structure of (A) Congo red, (B) Methyl ornage, (C) Methylene Blue, (D) Rhodamine 6g, (E) Rhodamine B and F curcumin.

photo-catalysis, advanced oxidation, coagulation, membrane filtration, flocculation-solidification, electrochemical practices, and adsorption. Among them all, adsorption is the most suitable one in terms of cost, simplicity, ecofriendliness, and efficiency [2,3,41].

Congo red (CR) is one of the anionic dyes with a pKa equal to 4.5. When it breaks down, it develops carcinogenic properties and mutagenic activities in aquatic ecosystems [4]. Methyl orange (MO) is a different anionic azo dye. It is also carcinogenic, toxic and mutagenic, and it lasts for a long time in the environment [5].

Moving on to another type of dyes, the cationic organic dyes, methylene blue (MB) is highly important because it can initiate vomiting, diarrhea, nausea, and breathing difficulties. It blocks the passage of solar radiations into water affecting by that the amount of oxygen necessary for the aquatic life [6]. Rhodamine 6G (Rh6G) is one more toxic cationic organic dye that has bad consequences related to the eyes and respiratory system. If rhodamine 6G contaminated water is drunk, it can provoke skin irradiation as well as cancer [7]. Likewise, rhodamine B (RhB) is a basic cationic dye utilized as a water tracer fluorescent molecule. It can cause irritation of skin and eyes as well as respiratory problems [8]. Therefore, developing an efficient complex for the adsorption process was taken into consideration. The structures of CR, MO, MB, Rh6G, and RhB are depicted in Fig. 1A–E respectively. Several materials were used for the treatment of wastewater and the adsorption of organic pollutants such as carbon nitride C_3N_4 photocalyst [9]; granular sludge [10], perovskites [11]; metal organic frameworks [12]; amidoxime/carbon nitride (AO/g-C_3N_4) [13]; fibrous adsorbent (PAN-F-TETA-PT) [14]; etc.

Lately, nanoscience has grown and been applied in many areas such as agriculture, cancer, environmental science, engineering, and drug delivery. Metal oxide nanoparticles have been considered as nutrition supplements that have the ability to go directly into the digestive system. They are capable of absorbing UV light and possess antimicrobial properties that permit their usage in food packaging [15]. Moreover, they are widely used in solar cells, sensing, photocatalytic applications, and electronics due to their vast surface area [16]. Their size ranges between 1 and 100 nm [17].

In this study, zinc oxide nanoparticles (ZnO NPs) were selected because of their varied biomedical applications. They are non-toxic in addition to exhibiting antimicrobial and anticancer activities [16]. ZnO NPs are as well determined to be semiconductors having their own and unique optical and electronic properties with a high exciton binding energy (60 meV) and a wide band gap (3.37 eV) [18]. These nanoparticles were chosen to be complexed with curcumin in order to enhance their activity. Curcumin is a bright yellow compound extracted from *Curcuma Longa* plant also called "turmeric" [19]. Methoxy and phenolic hydroxyl groups, double conjugated bonds, and bis-α,β-unsaturated β-diketone, are present in curcumin's molecular structure and are responsible for its medicinal and therapeutic potential (See Fig. 1F). This polyphenolic compound exhibits hydrophobic properties [20]. Lately, curcumin has been used as reducing agent and conjugating agent for metallic nanoparticles and metal oxide nanoparticles [21,22].

For this reason, in this word curcumin was used as a conjugated agent with zinc oxide nanoparticles to form a complex in order to obtain zinc curcumin oxide nanoparticles (Zn(Cur)O NPs) that will be used as adsorbent with a large and efficient surface area for the adsorption process of organic dyes. The pH of the solution will be varied to study its effect on the adsorption of different dyes onto the surface of the adsorbent nanoparticles.

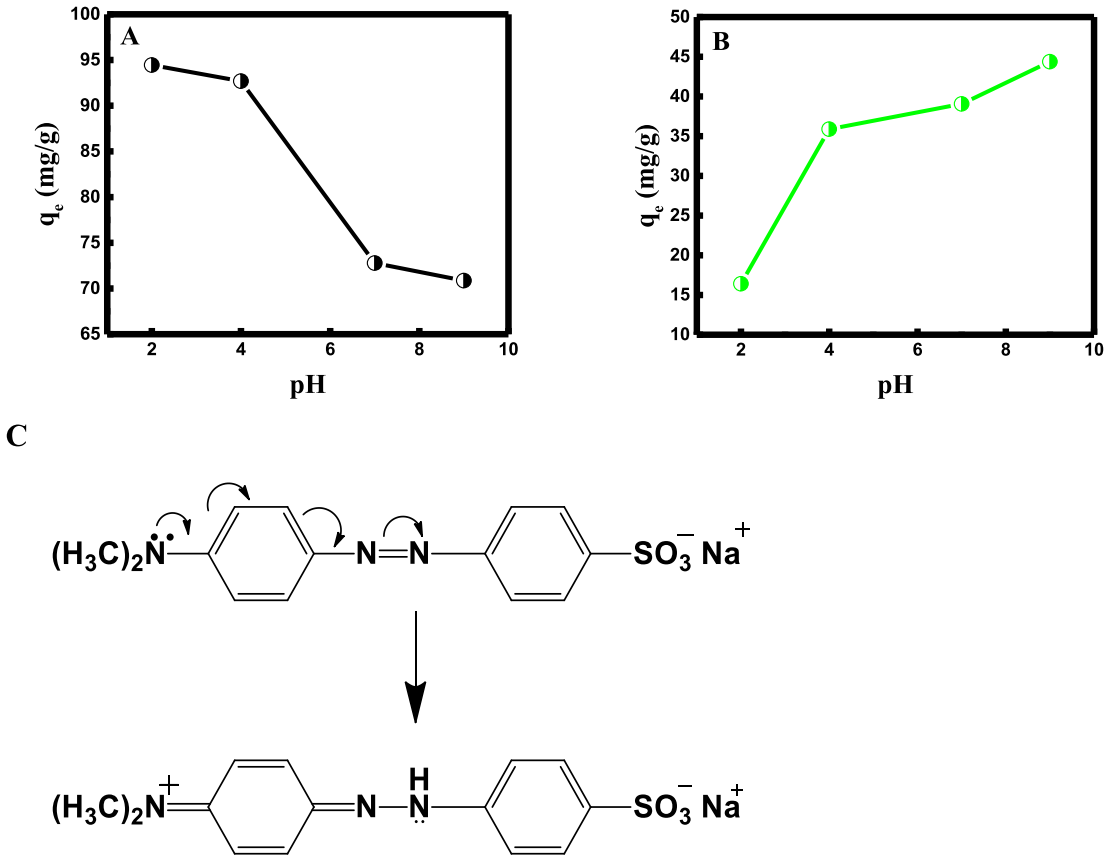

Fig. 2. Adsorption capacity of zinc curcumin oxide nanoparticles for (A) congo red removal; (B) methyl orange removal at different pH and (C) aspects of methyl orange in basic media. (For interpretation of the references to color in this figure legend, the reader is referred to the Web version of this article.)

2. Materials and methods

2.1. Materials

All the chemicals were used as received without any further purification. As for the source of the chemicals congo red, methyl orange, methylene blue, rhodamine 6G, rhodamine B and zinc nitrate hexahydrate ($Zn(NO_3)_2.6H_2O$) (98% extra pure) were purchased from Acros Organics. Curcumin was obtained from Sigma. Potassium hydroxide was gotten from AnalaR. Acetone (HPLC grade) was received from Aldrich. Sodium hydroxide and hydrochloric acid were acquired from Sigma Aldrich. The different organic dyes were dissolved in double distilled water while curcumin was dissolved in acetone obtained from Sigma Aldrich.

2.2. Methods

2.2.1. Zinc curcumin oxide nanoparticles synthesis

The synthesis of Zn(Cur)O NPs was done based on our previous optimized synthesis [23]. An amount of 1.48 g of zinc nitrate hexahydrate was dissolved in 50 mL pH = 13 solution heated at 80 °*C* (C = 0.1 M). In a separate tube 0.18 g of curcumin were dissolved in 5 mL of acetone (C = 0.1 M). The two solutions were mixed and set under reflux at 80 °*C* with constant stirring for 1 h. A solution of potassium hydroxide (C = 0.2 M) was prepared by dissolving 0.11 g of KOH in 10 mL (pH = 13) solution heated at 80 °*C*. It was added to the mixture after reflux drop by drop using a burette with constant stirring as well. Finally the solution was centrifuged at 4000 rpm for 10 min and the precipitate was washed 3 times with distilled water in order to get rid of the unreacted curcumin. The precipitate was freeze dried for 24 h to get a water soluble powder.

2.2.2. Preparation for the adsorption of organic dyes experiments

Organic dyes solutions (C = 1 mM) were prepared as follows:

Different amounts of 3.48 mg congo red, 1.64 mg methyl orange, 1.6 mg methylene blue, 2.36 mg rhodamine 6G, and 2.4 mg rhodamine B were dissolved each in 5 mL double distilled water.

For each adsorption experiment, 1 mL of double distilled water was heated and 1 mg of Zn(Cur)O NPs was dissolved in it using a sonicator to guarantee a complete dissolution of Zn(Cur)O NPs.

The organic dyes concentrations and the adsorbent dose were fixed to be 50 μM (150 μL) and 0.9 mg/mL (900 μL) respectively. The solutions of different pH were prepared using 0.1 M NaOH and 0.1 M HCl solutions. For each dye, the experiments were performed at four different pH. For the anionic dyes, pH = 2, 4, 7, and 9 were considered. As for the cationic dyes, the adsorption study was done at pH = 4, 7, 9, and 11.

2.3. Spectroscopic analysis and characterization techniques

The adsorption experiment was studied by measuring the absorbance of the solution within time. The absorption spectra were collected at room temperature utilizing a JASCOV-570 UV–vis–NIR Spectrophotometer in a range of 250–800 nm.

3. Results and discussion

3.1. Effect of pH on the adsorption

The pH of the solution is an important parameter that affects the whole adsorption process. It can modify the surface charge of the adsorbent. By doing that, the interactions between the organic dye and the adsorbent nanoparticles will vary between attraction and repulsion.

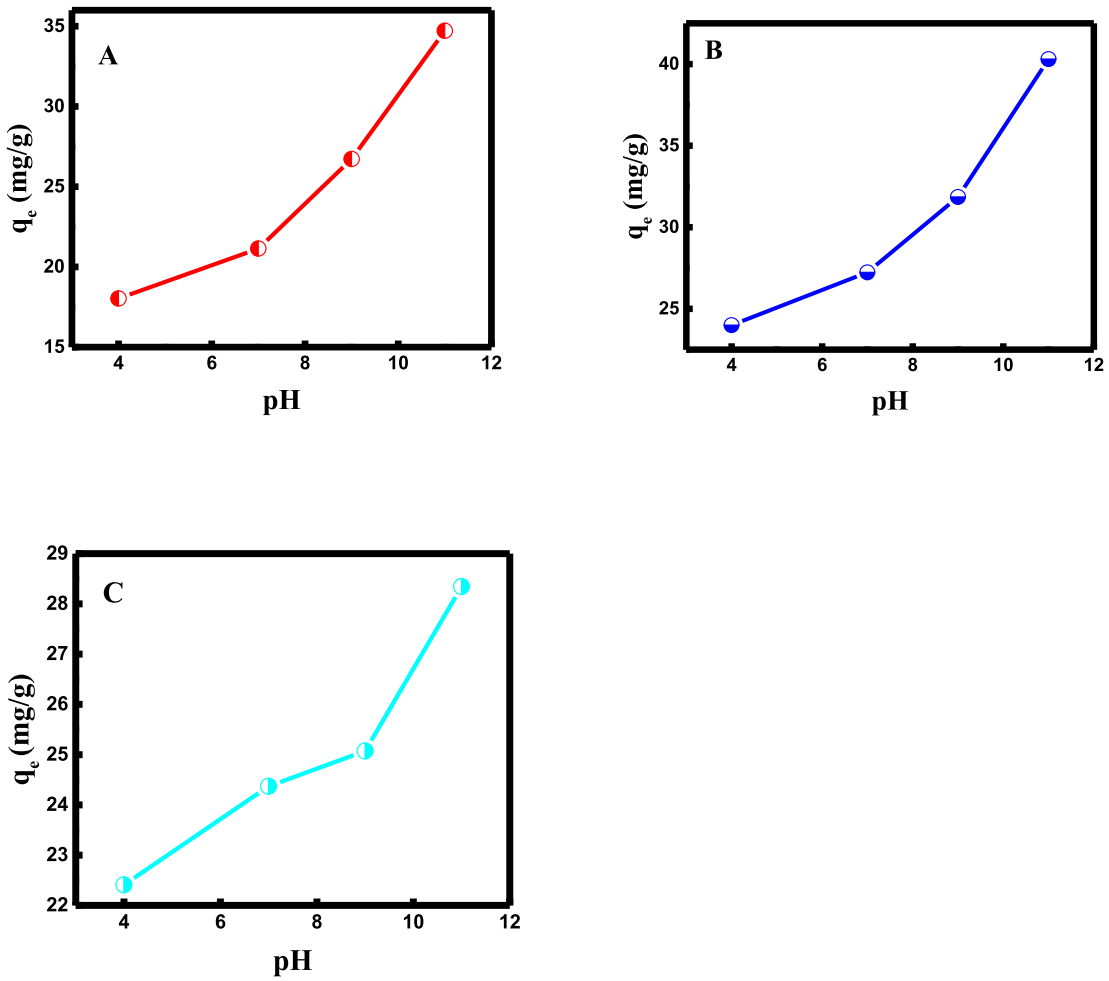

Fig. 3. Adsorption capacity of zinc curcumin oxide nanoparticles for (A) methylene blue removal; (B) for Rhodamine 6G removal and (C) for Rhodamine B removal at different pH. (For interpretation of the references to color in this figure legend, the reader is referred to the Web version of this article.)

Consequently, the adsorption capacity will decrease or increase with increasing the pH, depending on the nature of the organic dye, being anionic or cationic, and its interaction with Zn(Cur)O NPs [24,25].

3.1.1. Anionic dyes

3.1.1.1. Congo red. Anionic congo red is a di-azo organic dye, containing two N=N groups, having a molecular weight of 696.68 g/mol and a chemical formula of $C_{32}H_{22}N_6Na_2O_6S_2$. The two UV–Visible absoprtion peaks obtained at 344 nm and 497 nm correspond to the naphthalene ring and azo groups respectively [26]. The structure of congo red is characterized by the presence of two sulfonate functional groups $R–SO_3^-$. At highly acidic pH (pH = 2), the color of the solution turns from dark red into dark blue. In addition, the surface charge of Zn (Cur)O NPs becomes positively charged. Therefore, the negatively charged sulfonate group of congo red could be complexed with the positively charged adsorbent molecule by the zinc due to the high electrostatic attraction forces between them. This will make the adsorption capacity high. It will decrease with increasing the pH because of the repulsive interactions between the negative sulfonate groups and the negatively charged nanoparticles at high basic pH. This was proven in Fig. 2A where the adsorption capacity decreases with the increasing of the pH from $q_e = 94.54$ mg/g at pH = 2 to $q_e = 70.86$ mg/g at pH = 9.

3.1.2. Methyl orange

Another anionic organic dye is methyl orange. Its chemical formula is $C_{14}H_{14}N_3NaO_3S$ and molecular weight 327.33 g/mol. It is a part of the azo dyes family due to the presence of an azo group N=N in its chemical structure. Since it is an anionic dye also, it should be expected to behave like congo red organic dye at acidic and basic pH. From the structure of MO, there is a sulfonate group $R–SO_3^-$ in addition to an amine group $R–N(CH_3)_2$. Logically, the negatively charged sulfonate should be attracted to the positively charged Zn(Cur)O NPs at acidic pH, and this attraction should decrease gradually at higher pH, leading to a decrease in the adsorption capacity.

Surprisingly, this was not determined experimentally in that case. As we can notice in Fig. 2B, the adsorption capacity interestingly increases with the pH from 16.41 mg/g at pH = 2–44.38 mg/g at pH = 9. This is due to the presence of the amine group having a lone pair on the nitrogen atom that is able to be delocalized at basic pH on two N atoms as shown in the in Fig. 2C, hence increasing the probability of binding between the lone pair on the two nitrogen atoms and the zinc of the nanoparticles adsorbent. Further, Na^+ is present in methyl orange. In acidic medium, in competes with H^+ ions and the positively charged surface of the adsorbent, leading to a decrease in the adsorption capacity [27].

3.1.3. Cationic dyes

3.1.3.1. Methylene blue. Moving on to the cationic organic dyes, methylene blue having a chemical formula of $C_{16}H_{18}ClN_3S$, its molecular weight is 319.86 g/mol. It absorbs at $\lambda_{max} = 664$ nm. Since methylene blue is a cationic dye, it is predictable that the adsorption capacity

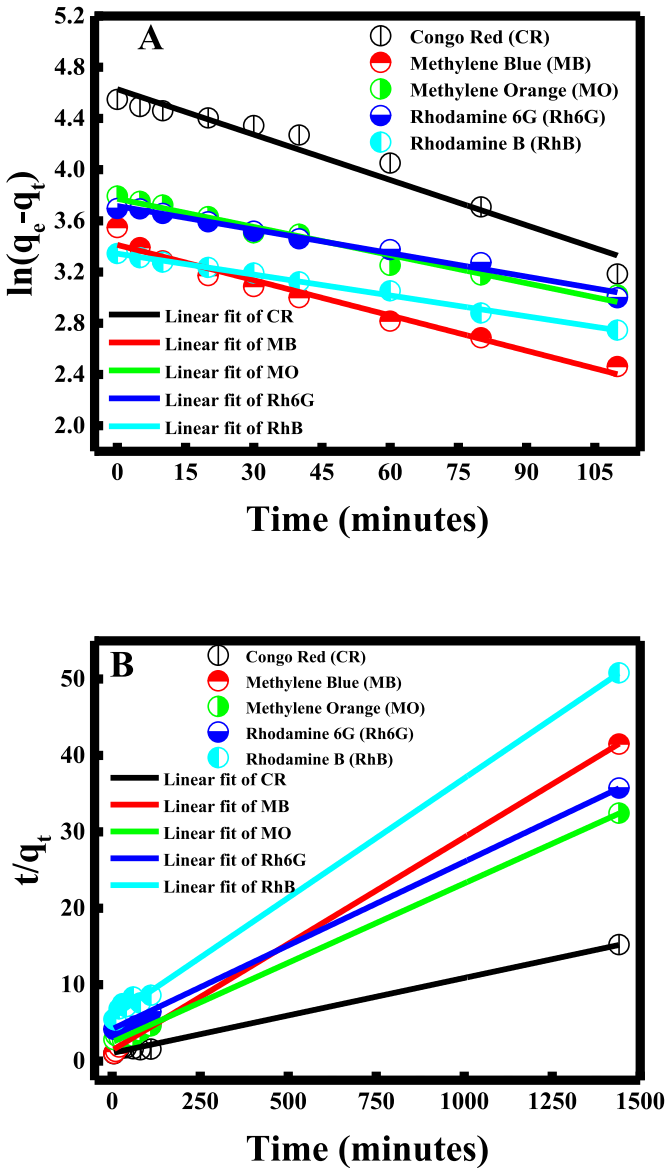

Fig. 4. Kinetics study (A) pseudo first order and (B) pseudo second order model.

should increase with increasing the pH. The results obtained prove the presence of higher interactions between the positively charged dye and the negatively charged adsorbent at basic pH. The adsorption capacity q_e improved from 18.02 to 34.71 mg/g when the pH changed from 4 to 11 as depicted in Fig. 3A. This is explained by the fact that the attraction forces increase between the two opposing charges of the dye and the adsorbent, enhancing by that the adsorption. In fact, another factor should also be taken into consideration, which is the presence of the π-π interactions between the nanoparticles and the aromatic ring of the organic dye. At acidic pH, there is less adsorption only due to the π-π interactions with the absence of the attraction and the presence of repulsion between two positively charged species [28].

3.1.3.2. Rhodamine 6G. Furthermore, rhodamine 6G is also a cationic dye. It is called also "rhodamine 590" and has a chemical formula of $C_{28}H_{31}N_2O_3Cl$ with a molecular weight of 479.02 g/mol. The maximum absorption peak is located at a maximum wavelength of around 530 nm [29]. The adsorption capacity increased from 23.99 mg/g to 38.184 mg/g when the pH varied from 4 to 11 (Fig. 3B). This is true due to the fact that the electrostatic attractions increased between the negative surface charge of zinc curcumin oxide nanoparticles and the cationic dye, allowing more adsorption onto the surface of the adsorbent.

Table 1A
pseudo first order kinetics and the relative K_1 and adsorption capacity value.

Organic Dye	Pseudo-first order			
	q_e (exp) (mg/g)	k_1 (min^{-1})	R^2	q_e (calc) (mg/g)
Congo Red	102.3297	0.01181	0.9495	94.4428
Methyl Orange	43.4851	0.00733	0.9752	44.3828
Methylene Blue	30.3328	0.00919	0.9660	34.7153
Rhodamine 6G	37.1788	0.00613	0.9851	40.3032
Rhodamine B	25.6286	0.00544	0.9890	28.3449

Table 1B
pseudo second order kinetics and the relative K_2 and adsorption capacity value.

Organic Dye	Pseudo-second order			
	q_e (exp) (mg/g)	k_2 ($g.mg^{-1}.min^{-1}$)	R^2	q_e (calc) (mg/g)
Congo Red	94.5179	$1.05237*10^{-4}$	0.99517	94.4428
Methyl Orange	44.6627	$2.02129*10^{-4}$	0.99863	44.3828
Methylene Blue	35.8937	$5.47555*10^{-4}$	0.99928	34.7153
Rhodamine 6G	40.8163	$1.43262*10^{-4}$	0.99986	40.3032
Rhodamine B	28.5796	$2.13981*10^{-4}$	0.99832	28.3449

3.1.3.3. Rhodamine B. The chemical formula of Rhodamine B is $C_{28}H_{31}ClN_2O_3$. Its molecular weight is 479.02 g/mol. The absorption peak is attained at λ_{max} around 543 nm [30]. Being as well cationic, it is expected to achieve higher adsorption at basic pH. This was demonstrated experimentally where the adsorption capacity q_e increased from 22.4 mg/g at pH = 4–28.34 mg/g at pH = 11 (Fig. 3C). This is not a very noticeable difference in the adsorption capacity between acidic and basic pH media compared to the previous organic dyes but it could be considered fine. Same as the other cationic organic dyes, the adsorption increases because of the attractive interactions between the negative surface charge of the adsorbent and the positive organic dye rhodamine B.

3.2. Kinetic studies

Kinetic studies of the adsorption of the different organic dyes onto the surface of zinc curcumin oxide nanoparticles were conducted. The results were plotted using the pseudo-first order and pseudo-second order kinetic model equations at a constant dye concentration of 50 μM and nanoparticles adsorbent amount of 0.9 mg:

$$\text{Pseudo} - \text{first order: } \ln(q_e - q_t) = \ln(q_e) - k_1 t \quad (1)$$

$$\text{Pseudo} - \text{second order: } \frac{t}{q_t} = \frac{1}{k_2 q_e^{\,2}} + \frac{1}{q_e} t \quad (2)$$

Knowing that q_e and q_t are the adsorption capacity at equilibrium and the adsorption capacity at time t respectively (mg/g), k_1 represents the rate constant of the pseudo-first order model (min^{-1}), k_2 indicates the rate constant of the pseudo-second order model ($g.mg^{-1}.min^{-1}$), and t signifies the time (min).

The plots of the pseudo-first and pseudo-second kinetic models that are used to study the adsorption process of the various dyes are demonstrated in Fig. 4A&B.

For the pseudo-first order, the values of the rate constant k_1 and the adsorption capacity at equilibrium q_e are calculated from the slope and the intercept, respectively (See Table 1A). Similarly, for the pseudo-second order, the rate constant k_2 is calculated from the intercept while the adsorption capacity at equilibrium q_e is calculated from the

Table 2
Different adsorbent use for the removal of the organic dyes.

Organic dye	Type and amount of adsorbent	Concentration of the dye (mg/mL)	q_e (mg/g)	References
Congo red	10 g/L of Pinus Pinaster Bark	5	0.47	[33]
	0.015 g of $Fe_{2.95}La_{0.05}O_4$	100	79.11	[34]
	0.9 mg of Zn(cur)O NPs	16	94.54	Our work
Methyl orange	50 mg of the β-CD/Fe_3O_4@PVP microspheres	13	47.62	[35]
	2g of chitosan/diatomite complex	50	35.12	[3]
	0.9 mg of Zn(cur)O NPs	16	44.38	Our work
Methylene blue	0.1 g of carbonized peanut shell	2.5	5.34	[36]
	0.2 g/L of biochar	50	20	[37]
	0.9 mg of Zn(cur)O NPs	16	34.71	Our work
Rhodamine 6G	10 mg/L of Fe_3O_4	6	150	[38]
	1 g/L of activated carbon	50	44.7	[39]
	0.9 mg of Zn(cur)O NPs	16	38.184	Our work
Rhodamine B	50 mg of seeds of *Aleurites Moluccana*	50	101	[40]
	0.9 mg of Zn(cur)O NPs	16	28.34	Our work

slope (See Table 1B). According to the obtained data, a remarkable difference was observed in the R^2 values of the two kinetic models of all the dyes, with the pseudo-second order having the greater values. This was also proven by Zhu et al. and Madan et al. [31,32].

Moreover, the experimental adsorption capacity values of the different organic dyes were approximately similar to the calculated adsorption capacity values in the pseudo-second order kinetic model with higher value of R^2, proving that the adsorption process of these dyes follows a pseudo-second order kinetic model. This means that the adsorption is done by chemisorption that requires the share of electrons between the zinc curcumin oxide nanoparticles adsorbent and the organic dyes. The efficiency of zinc curcumin oxide nanoparticles compared to different type of adsorbent is summarized in Table 2. It is obvious that in the majority of the adsorption experiments a minimum dose of 10 mg of the adsorbent is needed. Hence, only 0.9 mg of Zn(cur)O NPs were efficient to enhance the adsorption capacity of the dyes.

4. Conclusion

In conclusion, zinc curcumin oxide nanoparticles were synthesized in a simple green method. They were used as adsorbent for the adsorption process of organic dyes. Anionic dyes like congo red and methyl orange, in addition to cationic dyes such as methylene blue, rhodamine 6G and rhodamine B, were found to exhibit a successful adsorption process onto the surface of Zn(Cur)O NPs when using only 0.9 mg. The pH of the medium affected primarily the results due to the change in the surface charge of the nanoparticles based on the acidity and basicity. Consequently, the interactions between the organic dyes and the adsorbent were varied accordingly. Congo red was the only dye that has the highest adsorption capacity at an acidic pH, while the other dyes were better adsorbed in a basic medium. Finally, the adsorption process of all the dyes was found to follow a pseudo-second order kinetic model.

CRediT authorship contribution statement

Celine Arab: Methodology, Formal analysis, Investigation, Experiment, Validation, Writing – original draft, preparation. **Riham El Kurdi:** Formal analysis, Experiment, Analysis, Writing – review & editing. **Digambara Patra:** Conceptualization, Supervision, Resources, Project administration, Writing – review & editing.

Declaration of competing interest

The authors declare that they have no known competing financial interests or personal relationships that could have appeared to influence the work reported in this paper.

References

[1] N. Chaukura, E.C. Murimba, W. Gwenzi, Synthesis, characterisation and methyl orange adsorption capacity of ferric oxide–biochar nano-composites derived from pulp and paper sludge, Applied Water Science 7 (5) (2017) 2175–2186, https://doi.org/10.1007/s13201-016-0392-5.

[2] Y. Li, H. Wang, W. Zhao, X. Wang, Y. Shi, H. Fan, H. Sun, L. Tan, Facile synthesis of a triptycene-based porous organic polymer with a high efficiency and recyclable adsorption for organic dyes, J. Appl. Polym. Sci. 136 (39) (2019) 1–10, https://doi.org/10.1002/app.47987.

[3] J. Zhao, H.Y. Lin, G.C. Liu, X. Wang, X.L. Wang, Two Cu(II) coordination polymers based on a flexible bis(pyridyl-tetrazole): solvent-ratio induced various structures and distinct adsorption performance for organic dyes, Inorg. Chim. Acta. 464 (2017) 114–118, https://doi.org/10.1016/j.ica.2017.05.008.

[4] N.B. Swan, M.A.A. Zaini, Adsorption of malachite green and Congo red dyes from water: recent progress and future outlook, Ecol. Chem. Eng. 26 (1) (2019) 119–132, https://doi.org/10.1515/eces-2019-0009.

[5] M.J. Chatterjee, S.T. Ahamed, M. Mitra, C. Kulsi, A. Mondal, D. Banerjee, Visible-light influenced photocatalytic activity of polyaniline -bismuth selenide composites for the degradation of methyl orange, rhodamine B and malachite green dyes, Appl. Surf. Sci. 470 (2019) 472–483, https://doi.org/10.1016/j.apsusc.2018.11.085.

[6] M. Mahanthappa, N. Kottam, S. Yellappa, Enhanced photocatalytic degradation of methylene blue dye using CuS–CdS nanocomposite under visible light irradiation, Appl. Surf. Sci. 475 (2019) 828–838, https://doi.org/10.1016/j.apsusc.2018.12.178.

[7] U. Pal, A. Sandoval, S.I.U. Madrid, G. Corro, V. Sharma, P. Mohanty, Mixed titanium, silicon, and aluminum oxide nanostructures as novel adsorbent for removal of rhodamine 6G and methylene blue as cationic dyes from aqueous solution, Chemosphere 163 (2016) 142–152, https://doi.org/10.1016/j.chemosphere.2016.08.020.

[8] N. Nekouei Marnani, A. Shahbazi, A novel environmental-friendly nanobiocomposite synthesis by EDTA and chitosan functionalized magnetic graphene oxide for high removal of Rhodamine B: adsorption mechanism and separation property, Chemosphere 218 (2019) 715–725, https://doi.org/10.1016/j.chemosphere.2018.11.109.

[9] H. Wang, H. Guo, N. Zhang, Z. Chen, B. Hu, X. Wang, Enhanced photoreduction of U(VI) on C3N4 by Cr(VI) and bisphenol A: ESR, XPS, and EXAFS investigation [Research-article], Environ. Sci. Technol. 53 (11) (2019) 6454–6461, https://doi.org/10.1021/acs.est.8b06913.

[10] Y. Zhu, W. Wang, J. Ni, B. Hu, Cultivation of granules containing anaerobic decolorization and aerobic degradation cultures for the complete mineralization of azo dyes in wastewater, Chemosphere 246 (13) (2020) 1–10, https://doi.org/10.1016/j.chemosphere.2019.125753.

[11] Z.N. Garba, W. Zhou, M. Zhang, Z. Yuan, A review on the preparation, characterization and potential application of perovskites as adsorbents for wastewater treatment, Chemosphere 244 (19) (2020), https://doi.org/10.1016/j.chemosphere.2019.125474.

[12] M. Hao, M. Qiu, H. Yang, B. Hu, X. Wang, Recent advances on preparation and environmental applications of MOF-derived carbons in catalysis, Sci. Total Environ. (20) (2021) 760, https://doi.org/10.1016/j.scitotenv.2020.143333.

[13] B. Hu, H. Wang, R. Liu, M. Qiu, Highly efficient U(VI) capture by amidoxime/carbon nitride composites: evidence of EXAFS and modeling, Chemosphere 274 (2021) 1–9, https://doi.org/10.1016/j.chemosphere.2021.129743.

[14] F. Liu, Z. Zhou, G. Li, Persimmon tannin functionalized polyacrylonitrile fiber for highly efficient and selective recovery of Au(III) from aqueous solution, Chemosphere 264 (2021) 1–9, https://doi.org/10.1016/j.chemosphere.2020.128469.

[15] T. Schneider, M. Westermann, M. Glei, In vitro uptake and toxicity studies of metal nanoparticles and metal oxide nanoparticles in human HT29 cells, Arch. Toxicol. 91 (11) (2017) 3517–3527, https://doi.org/10.1007/s00204-017-1976-z.

[16] E.E. Elemike, D.C. Onwudiwe, M. Singh, Eco-friendly synthesis of copper oxide, zinc oxide and copper oxide–zinc oxide nanocomposites, and their anticancer applications, J. Inorg. Organomet. Polym. Mater. 30 (2) (2020) 400–409, https://doi.org/10.1007/s10904-019-01198-w.

[17] J. Sun, S. Wang, D. Zhao, F.H. Hun, L. Weng, H. Liu, Cytotoxicity, permeability, and inflammation of metal oxide nanoparticles in human cardiac microvascular endothelial cells: cytotoxicity, permeability, and inflammation of metal oxide nanoparticles, Cell Biol. Toxicol. 27 (5) (2011) 333–342, https://doi.org/10.1007/s10565-011-9191-9.

[18] J. Jassi, V. Biju, A. Shajan, Structural and optical properties of zinc oxide nanoparticles, AIP Conference Proceedings 2263 (1) (2020) 1–4, https://doi.org/10.1063/5.0017263.

[19] J. Li, I.W. Lee, G.H. Shin, X. Chen, H.J. Park, Curcumin-Eudragit® e PO solid dispersion: a simple and potent method to solve the problems of curcumin, Eur. J. Pharm. Biopharm. 94 (2015) 322–332, https://doi.org/10.1016/j.ejpb.2015.06.002.

[20] M.N. Oskouie, N.S. Aghili Moghaddam, A.E. Butler, P. Zamani, A. Sahebkar, Therapeutic use of curcumin-encapsulated and curcumin-primed exosomes, J. Cell. Physiol. 234 (6) (2019) 8182–8191, https://doi.org/10.1002/jcp.27615.

[21] R. El Kurdi, D. Patra, Tuning the surface of Au nanoparticles using poly(ethylene glycol)- block -poly(propylene glycol)- block -poly(ethylene glycol): enzyme free and label free sugar sensing in serum samples using resonance Rayleigh scattering spectroscopy, Phys. Chem. Chem. Phys. 20 (14) (2018) 9616–9629, https://doi.org/10.1039/c8cp01147h.

[22] M. Qasem, R. El Kurdi, D. Patra, Glutathione-capped CuO nanoparticles for the determination of cystine using resonance Rayleigh scattering spectroscopy, Microchimica Acta 187 (6) (2020) 1–8, https://doi.org/10.1007/s00604-020-04331-6.

[23] C. Arab, R. El Kurdi, D. Patra, Efficient removal of Congo red using curcumin conjugated zinc oxide nanoparticles as new adsorbent complex, Chemosphere 276 (2021) 1–9, https://doi.org/10.1016/j.chemosphere.2021.130158.

[24] H. Peng, S. Zhong, Q. Lin, X. Yao, Z. Liang, M. Yang, G. Yin, Q. Liu, H. He, Removal of both cationic and anionic contaminants by amphoteric starch, Carbohydr. Polym. 138 (2016) 210–214, https://doi.org/10.1016/j.carbpol.2015.11.064.

[25] W. Zhang, H. Yang, L. Dong, H. Yan, H. Li, Z. Jiang, X. Kan, A. Li, R. Cheng, Efficient removal of both cationic and anionic dyes from aqueous solutions using a novel amphoteric straw-based adsorbent, Carbohydr. Polym. 90 (2) (2012) 887–893, https://doi.org/10.1016/j.carbpol.2012.06.015.

[26] B.T. Gadisa, R. Appiah-Ntiamoah, H. Kim, Amorphous iron sulfide nanowires as an efficient adsorbent for toxic dye effluents remediation, Environ. Sci. Pollut. Control Ser. 26 (3) (2019) 2734–2746, https://doi.org/10.1007/s11356-018-3811-3.

[27] I. Mantasha, H.A.M. Saleh, K.M.A. Qasem, M. Shahid, M. Mehtab, M. Ahmad, Efficient and selective adsorption and separation of methylene blue (MB) from mixture of dyes in aqueous environment employing a Cu(II) based metal organic framework, Inorg. Chim. Acta. 511 (2020) 1–11, https://doi.org/10.1016/j.ica.2020.119787.

[28] M. Sharifi-Bonab, S. Aber, D. Salari, F. Khodam, Synthesis of CoZnAl-layered double hydroxide/graphene oxide nanocomposite for the removal of methylene blue : kinetic , thermodynamic , and isotherm studies, Environ. Prog. Sustain. Energy 39 (2) (2020) 1–12, https://doi.org/10.1002/ep.13316.

[29] I.T. Sugiarto, Isnaeni, K.Y. Putri, Analysis of dual peak emission from Rhodamine 6G organic dyes using photoluminescence, J. Phys. Conf. 817 (2017) 1–6, https://doi.org/10.1088/1742-6596/755/1/011001.

[30] A.A. Oyekanmi, A. Ahmad, K. Hossain, M. Rafatullah, Adsorption of Rhodamine B dye from aqueous solution onto acid treated banana peel: response surface methodology, kinetics and isotherm studies, PLoS One 14 (5) (2019) 1–20, https://doi.org/10.1371/journal.pone.0216878.

[31] S. Madan, R. Shaw, S. Tiwari, S.K. Tiwari, Adsorption dynamics of Congo red dye removal using ZnO functionalized high silica zeolitic particles, Appl. Surf. Sci. 487 (2019) 907–917, https://doi.org/10.1016/j.apsusc.2019.04.273.

[32] H.Y. Zhu, R. Jiang, J. Yao, F.Q. Fu, J.B. Li, Novel ZnO/Zn–Cr hydrotalcite-like anionic clay as a high-performance and recyclable material for efficient photocatalytic removal of organic dye under simulated solar irradiation, Res. Chem. Intermed. 42 (5) (2016) 4359–4372, https://doi.org/10.1007/s11164-015-2280-2.

[33] K. Litefti, M.S. Freire, M. Stitou, J. González-Álvarez, Adsorption of an anionic dye (Congo red) from aqueous solutions by pine bark, Sci. Rep. 9 (1) (2019) 1–11, https://doi.org/10.1038/s41598-019-53046-z.

[34] L. Wang, J. Li, Y. Wang, L. Zhao, Preparation of nanocrystalline Fe 3-xLa xO 4 ferrite and their adsorption capability for Congo red, J. Hazard Mater. 196 (2011) 342–349, https://doi.org/10.1016/j.jhazmat.2011.09.032.

[35] Q. Si, Q. Wen, Q. Yang, Y. Song, Y. Li, Preparation of β-cyclodextrin/Fe3O4/polyvinylpyrrolidone composite magnetic microspheres for the adsorption of methyl orange, Chem. Res. Chin. Univ. 33 (6) (2017) 1012–1016, https://doi.org/10.1007/s40242-017-7083-0.

[36] J. Gülen, F. Zorbay, Methylene blue adsorption on a low cost adsorbent—carbonized peanut shell, Water Environ. Res. 89 (9) (2017) 805–816, https://doi.org/10.2175/106143017x14902968254836.

[37] S.H. Kong, S.S. Lam, P.N.Y. Yek, R.K. Liew, N.L. Ma, M.S. Osman, C.C. Wong, Self-purging microwave pyrolysis: an innovative approach to convert oil palm shell into carbon-rich biochar for methylene blue adsorption, J. Chem. Technol. Biotechnol. 94 (5) (2019) 1397–1405, https://doi.org/10.1002/jctb.5884.

[38] S. Phoemphoonthanyakit, P. Seeharaj, P. Damrongsak, K. Locharoenrat, Effect of adsorption characteristics of rhodamine 6G dye solution in Fe3O4 magnetic nanoparticles on fluorescence Quantum Yield, J. Spectrosc. (2019) 1–5, https://doi.org/10.1155/2019/2853989, 2019.

[39] G. Annadurai, R.S. Juang, D.J. Lee, Adsorption of rhodamine 6G from aqueous solutions on activated carbon, J. Environ. Sci. Health. - Part A Toxic/Hazardous . Subst. Environ. Eng. 36 (5) (2001) 715–725, https://doi.org/10.1081/ESE-100103755.

[40] D.L. Postai, C.A. Demarchi, F. Zanatta, D.C.C. Melo, C.A. Rodrigues, Adsorption of rhodamine B and methylene blue dyes using waste of seeds of Aleurites Moluccana, a low cost adsorbent, Alexandria Engineering Journal 55 (2) (2016) 1713–1723, https://doi.org/10.1016/j.aej.2016.03.017.

[41] P. Zhao, R. Zhang, J. Wang, Adsorption of methyl orange from aqueous solution using chitosan/diatomite composite, Water Sci. Technol. 75 (7) (2017) 1633–1642, https://doi.org/10.2166/wst.2017.034.